A Penning trap mass spectrometer for the study of cluster ions

St. Becker[a)]
Institut für Physik, Johannes Gutenberg-Universität, D-55099 Mainz, Germany

K. Dasgupta
Bhabha Atomic Research Center, Bombay 400085, India

G. Dietrich
Institut für Kernchemie, Johannes Gutenberg-Universität, D-55099 Mainz, Germany

H.-J. Kluge[b)]
Institut für Physik, Johannes Gutenberg-Universität, D-55099 Mainz, Germany

S. Kuznetsov
Department of Chemistry, Moscow State University, 119899 Moscow, Russia

M. Lindinger
Institut für Physik, Johannes Gutenberg-Universität, D-55099 Mainz, Germany

K. Lützenkirchen
Institut für Kernchemie, Johannes Gutenberg-Universität, D-55099 Mainz, Germany

L. Schweikhard and J. Ziegler
Institut für Physik, Johannes Gutenberg-Universität, D-55099 Mainz, Germany

(Received 11 April 1995; accepted for publication 27 June 1995)

A Penning trap system has been set up for storing and investigating cluster ions over time ranges from microseconds up to minutes. This enables studies of cluster reactions with extremely low cross sections and the observation of their time dependence in a new regime. The ions are created externally by laser vaporization, cooled by adiabatic expansion of a supersonic beam, and injected into the Penning trap. Detection of reaction products is achieved by combining the advantages of two complementary approaches, viz. the high resolution of Fourier transform mass spectrometry and the high sensitivity of single-ion counting with a time-of-flight mass spectrometer. The performance of the apparatus is illustrated by results of recent cluster experiments. © *1995 American Institute of Physics.*

I. INTRODUCTION

Atomic clusters offer the unique possibility to study the evolution of physical properties from an atomic scale up to bulk dimensions. Commonly, cluster experiments in the gas phase are carried out with particle beams. This imposes an upper limit to the time scale of the observable processes in the order of milliseconds. For many experiments this is not a drawback, since the relevant characteristic times for the decay of electronic into vibrational excitations are well below this limit.[1] On the other hand, other de-excitation processes of excited clusters, like the emission of atoms, electrons, or electromagnetic radiation, may require times much larger than a millisecond. Also, for the study of reactions with small cross sections or in the case of a low density of the ion species under investigation, like for cluster–cluster collisions, long interaction periods up to many seconds are mandatory. The appropriate instrument to carry out these types of experiments is an ion trap which allows the storage of clusters.

Ion trapping devices[2] have gained more and more importance in the last two decades in physics[3,4] and chemistry.[5,6] As demonstrated for a single stored electron, charged particles can be investigated for extended periods of time up to seconds, minutes, or even up to several months.[7] This long storage time is the key to accuracy as shown, e.g., in the case of the g-2 measurement of the electron and positron[8] and mass determinations of stable[9–11] and unstable isotopes[12] or of the antiproton.[13] Also, chemical reactions of metal ions[14] and cluster ions,[15,16] as well as low-temperature ion–molecule reactions related to interstellar chemistry,[17] have been studied.

The two most important ion trapping systems are the Penning [ion cyclotron resonance (ICR)] trap and the Paul or radio frequency (rf) trap. In the latter the mass range of the ions stored is selected by the applied rf and dc voltages,[18,19] in the Penning trap all masses below a critical size are stored by superposition of a homogeneous magnetic and a dc electric field.[20] If ions of high mass-to-charge ratio (e.g., clusters) are to be stored in an ICR trap the magnetic field must be high. Therefore superconducting magnets are used to supply the magnetic field. The presence of the magnetic field can be exploited for mass spectrometric analysis of the stored ion ensemble by the measurement of their cyclotron frequencies. With Fourier transform–ion cyclotron resonance (FT–ICR) high resolving powers are achieved over a broad mass range.[21] However, even under favorable experimental conditions the number of (singly charged) ions required for a detectable signal is in the order of several hundred (see below). High-sensitivity detection of single particles, on the other

[a)]Present address: iC-Haus, Am Kuemmerling 18, D-55294 Bodenheim, Germany.
[b)]Present address: GSI Darmstadt, Postfach 110 552, D-64220 Darmstadt, Germany.

 0034-6748/95/66(10)/4902/9/$6.00 © 1995 American Institute of Physics

Downloaded 14 Mar 2003 to 137.138.124.154. Redistribution subject to AIP license or copyright, see http://ojps.aip.org/rsio/rsicr.jsp

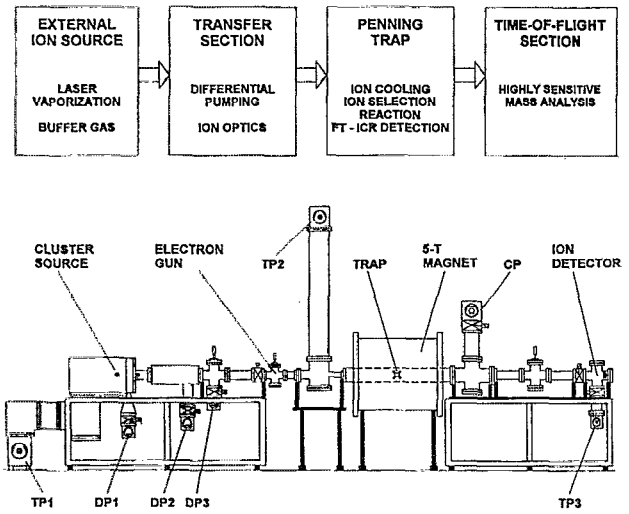

FIG. 1. Top: Overview of the major parts of the experimental setup. Bottom: Schematic diagram of the vacuum system. TP1–TP3 are turbomolecular pumps, DP1–DP3 are diffusion pumps, and CP is a cryopump. For details see text.

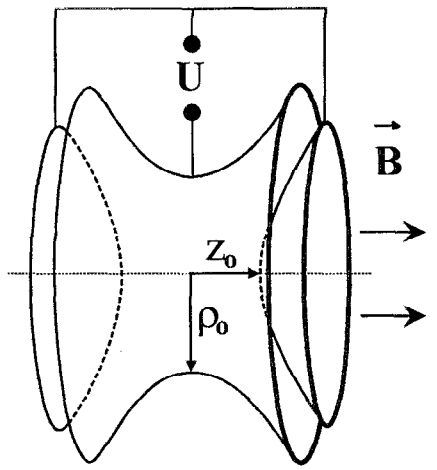

FIG. 2. Schematic diagram of the Penning trap which consists of hyperbolically shaped electrodes, two endcaps, and one ring electrode. Storage of ions is achieved with a magnetic field along the z axis and an electric quadrupole potential produced by the voltage U between the endcaps and the ring electrode.

hand, is easily achieved with a channeltron or channelplate arrangement which is typical of time-of-flight (TOF) experiments.

In this work we present a Penning trap system for the study of cluster ions that includes external ion injection and ion analysis by FT–ICR and TOF mass spectrometry. The apparatus described here operates with a Penning trap, i.e., an ICR trap with hyperbolically shaped electrodes. The experimental approach and an overview of the entire setup is given in Fig. 1. It consists of the following sections:

Cluster ion source: A prerequisite for the formation of atomic clusters is efficient cooling which is achieved by collisions with rare gas atoms followed by an adiabatic expansion of the cluster-rare gas mixture. This method of cluster production requires the use of an external ion source which is separated from the ultrahigh vacuum region of the Penning trap.

Transfer section: After their formation, the charged clusters are guided towards the Penning trap through a transfer section which consists of several stages for differential pumping and ion-optical elements.

Penning trap: Once being captured in the trap, clusters may be cooled to room temperature by collisions with a buffer gas. Also, a single and well-defined cluster size may be prepared by radial ejection of unwanted ion species via excitation of their cyclotron motion. After interactions with, e.g., photons or neutral molecules, reaction products are identified through mass analysis. Given a sufficient number of ions, the system holds the possibility to perform FT–ICR detection of the ions while they stay inside the trap.

TOF section: Complementary, ions may be axially ejected and mass analyzed in a TOF section. With this arrangement the advantages of FT–ICR and TOF, high resolution and high sensitivity, are combined. Recently, a setup has been reported, which combines a rf trap with TOF analysis.[22] However, in this case the ions have been created inside the trap and ICR excitation and/or detection is not possible.

II. ION TRAP

The central part of the apparatus is the Penning trap.[20] Ion storage is achieved by superposition of a homogeneous 5-T magnetic field provided by a superconducting magnet (Oxford Instruments, 5T/183) and an axial quadrupolar electric field. Both fields are static, as opposed to the electric-only rf trap. The Penning trap consists of hyperbolically shaped electrodes, one ring and two endcap electrodes (Fig. 2). Each endcap has a 5-mm hole in the center in order to inject (eject) the externally created clusters into (out of) the trap. The ring electrode is divided into eight segments[23,24] for rf excitation and detection of ion motions. The minimum distances from the ring electrode and the endcap electrodes to the center of the trap are $\rho_0=20$ mm and $z_0=\rho_0/\sqrt{2}$ (asymptotically symmetric trap). With potentials ϕ_{EC} and ϕ_R of the endcap and the ring electrodes the resulting trap potential[25,26] is given by

$$\phi(x,y,z)=\frac{\phi_{EC}+\phi_R}{2}+\frac{\phi_{EC}-\phi_R}{4d^2}(2z^2-x^2-y^2). \quad (1)$$

The parameter $d^2=(z_0^2+\rho_0^2/2)/2$ reflects the spatial dimensions of the trap.[20] From Eq. (1) the depth of the potential well along the z axis follows as

$$U_T=\phi(0,0,z_0)-\phi(0,0,0)=U/2, \quad (2)$$

where U is the trapping voltage applied between the endcaps and the ring, $U=\phi_{EC}-\phi_R$. The electric quadrupole field leads to an axial harmonic oscillation of the trapped ions between the endcaps, known as trapping motion, or z motion. The trapping frequency

$$\nu_z=\frac{1}{2\pi}\sqrt{\frac{qU}{md^2}} \quad (3)$$

depends on the trap potential U, the charge-to-mass ratio q/m, and the trap dimension parameter d^2. Perpendicular to the magnetic field the ions perform the circular cyclotron motion. Its frequency in the absence of an electric field

Downloaded 14 Mar 2003 to 137.138.124.154. Redistribution subject to AIP license or copyright, see http://ojps.aip.org/rsio/rsicr.jsp

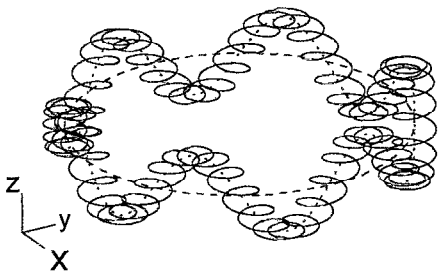

FIG. 3. Ion trajectory in the Penning trap. Dashed line: Magnetron motion only. Dotted line: Combined magnetron and axial trapping motion. Solid line: Full ion motion, i.e., combined magnetron, axial trapping, and cyclotron motion. Note that the drawing is schematic and does not represent the frequency relations as given in Eq. (6). For a detailed description see Ref. 30.

$$\nu_c = \frac{1}{2\pi}\frac{q}{m}B \tag{4}$$

is a function of the charge-to-mass ratio q/m, and the magnetic field B. In the presence of an electric trapping field the frequency of the cyclotron motion decreases. It is therefore referred to as the reduced cyclotron frequency, ν_+. Furthermore, there is a second circular motion, the magnetron motion with frequency ν_-, a drift motion perpendicular to both the magnetic and the electric field. The reduced cyclotron frequency and the magnetron frequency can be expressed via the cyclotron and trapping frequencies by

$$\nu_\pm = \frac{\nu_c}{2} \pm \sqrt{\frac{\nu_c^2}{4} - \frac{\nu_z^2}{2}}. \tag{5}$$

The eigenfrequencies are related by

$$\nu_+ \nu_- = \frac{\nu_z^2}{2}. \tag{6}$$

Apart from field imperfections, the frequencies of the three types of ion motion are independent of the respective amplitudes due to the quadrupole geometry of the electric field throughout the entire Penning trap volume. The ion trajectory in a Penning trap is illustrated in Fig. 3. Table I gives an overview of the frequencies of the ion motion for an atomic gold ion and the clusters Au_{10}^+ and Au_{100}^+.

III. CLUSTER ION SOURCE

A versatile technique to produce clusters of refractory elements is laser vaporization[27] into a helium gas followed by adiabatic expansion. The gas load of the cluster source requires it to be located at some distance from the ultrahigh vacuum region of the Penning trap. The laser vaporization source in use was constructed by Weidele *et al.*[28] The 532-nm beam of a Q-switched Nd:YAG laser (Lumonics HY400, pulse energy 1–20 mJ, repetition rate 10 Hz) is focused onto a metal wire of 0.5 mm (or 1.0 mm) diameter. Every 200 to 1000 laser shots the wire is pulled a distance of 0.1 mm by a stepping motor to prevent hole drilling by the laser pulses. About 1 ms prior to the laser pulse, a helium pulse (duration 300–400 μs, stagnation pressure 4 bar) is injected into the vaporization chamber through a solenoid valve (General Valve Corp.). Neutral and ionized clusters are formed in the helium atmosphere and are subsequently cooled during an adiabatic expansion through a nozzle of 10 mm length with a diameter in the range from 0.3 to 1.2 mm.

In order to perform experiments with cold cluster ions no postionization of the (more abundant) neutral species in the supersonic beam is used. Instead, the directly produced positive (negative) ions are extracted from the laser-produced plasma through the nozzle by a potential of +100 V (−100 V) applied to the cluster source. As the transfer section is on ground potential, the clusters thereby acquire a kinetic energy of 100 eV. Due to the collisions with helium atoms during the adiabatic expansion the total kinetic energy is, however, somewhat higher and increases with cluster size. For gold clusters, Au_n^+, a kinetic energy of approximately $(100+1.7\times n)$ eV was determined by use of a retardation potential.[29] Singly charged gold clusters of up to 145 atoms, i.e., $m=28\ 560$ amu, were produced in the external source, transferred, and stored in the trap.[30]

Experiments with ions of gaseous atoms or molecules do not require an external source. Instead, ions may be generated inside the Penning trap by electron impact ionization with an electron gun that is installed in the transfer section 1.2 m in front of the Penning trap. It consists of a rhenium filament, which is heated by a current of 3–4 A and placed on a potential some tens of volts below the one of the entrance endcap. An example for the use of electron impact ionization is the determination of the absolute pressure inside the Penning trap. This was achieved by ionizing CH_4 and measuring the pressure dependent pseudo-first-order rate constant of the reaction $CH_4^+ + CH_4 \rightarrow CH_5^+ + CH_3$.[31] Knowledge of the pressure is a prerequisite for measuring absolute rates of ion-molecule reactions.

TABLE I. Eigenfrequencies of the ion motion (the reduced cyclotron frequencies, ν_+, the trapping frequencies, ν_z, and the magnetron frequencies, ν_-) for Au^+, Au_{10}^+, and Au_{100}^+ for a magnetic field of $B=5$ T, a trapping voltage of $U=10$ V, and a trap parameter of $d^2=200$ mm^2.

Cluster ion	ν_+ (kHz)	ν_z (kHz)	ν_- (kHz)
Au^+	389.024	24.908	0.797
Au_{10}^+	38.169	7.877	0.813
Au_{100}^+	2.784	2.491	1.114

IV. ION TRANSFER AND CAPTURE

The ion-transfer part (Fig. 4) consists of four differentially pumped sections, separated by skimmers and apertures, which results in pressure in the Penning trap region of $p<10^{-8}$ mbar. The cluster beam is guided towards the Penning trap using three arrays of electrostatic lenses and deflectors. In order to reduce the conversion of axial energy into cyclotron energy, the beam is transported in the fringe field of the magnet as parallel as possible to the magnetic field lines. In-flight capture[32] of clusters is performed by lowering the potential of the entrance endcap from ϕ_{EC} down to ϕ_R when the ions are arriving and increasing it back to the trapping value ϕ_{EC} when they are inside the trap (Fig. 5).

Since the kinetic energies of clusters increase with size, the injection process is mass selective. Applying potentials of

Downloaded 14 Mar 2003 to 137.138.124.154. Redistribution subject to AIP license or copyright, see http://ojps.aip.org/rsio/rsicr.jsp

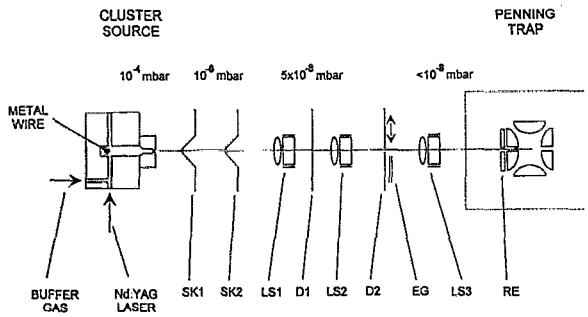

FIG. 4. Outline of the laser vaporization source and the ion-transfer section consisting of four differentially pumped sections, separated by skimmers (SK) and diaphragms (D). The typical pressure in each section is indicated. LS: ion-optical lenses and steerers; EG: electron gun; RE: retardation electrode.

ϕ_R to the entrance endcap and ϕ_{EC} to the exit endcap during ion injection, cluster ions with kinetic energies between $q\phi_R$ and $q\phi_{EC}$ can be captured [e.g., Au_{19}^+ to Au_{24}^+ in Fig. 6(a)].

Due to the finite length of the Penning trap, only a fraction of one cluster bunch can be captured. An estimate of this fraction is given by the ratio of the residence time of clusters in the trap during injection, which corresponds to the period T_z of the axial trapping motion, and the temporal length of the cluster bunch. Depending upon cluster size, a length of 1–2 ms was determined by varying the time delay between cluster production and capture. For Au_{10}^+ ions with $T_z \cong 100$ μs and a bunch length of about 1 ms the resulting trapping efficiency is 10%. Typically, 10–100 cluster ions of a single size are captured for each pulse of the vaporization laser. This number was obtained by axial ejection of ions from the trap and detection via TOF mass spectrometry (see below).

V. ION SEPARATION AND PREPARATION

Most experiments with clusters require a single, well-defined cluster size to be present in an interaction region for unambiguous identification of the reaction channels. Hence, the captured cluster bunch [Fig. 6(a)] needs to be further mass separated. A single cluster size is prepared by rf excitation of the reduced cyclotron motions of all other ions at their cyclotron frequencies ν_+ [Eq. (5)]. The excited ions eventually collide with the ring electrode, whereas the selected cluster species stay within the trap [Fig. 6(b)]. For rf

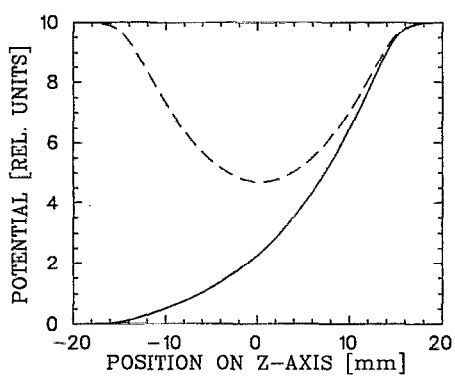

FIG. 5. Penning trap potentials during ion injection (solid line) and storage (dashed line).

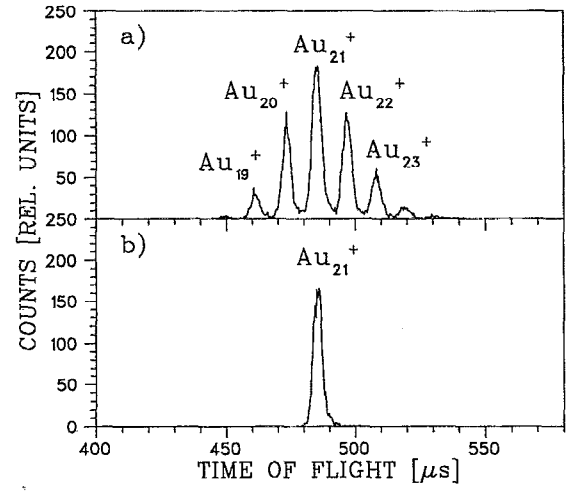

FIG. 6. Time-of-flight spectra showing the mass separation of clusters in the Penning trap. (a) The mass range of captured cluster ions as selected by the potentials applied to the trap electrodes. (b) Preparation of a single cluster size. All other ions are radially ejected by rf excitation of their cyclotron motions.

excitation the SWIFT technique[33] is used: Frequency spectra corresponding to the mass ranges to be ejected are calculated and subjected to an inverse Fourier transformation. The resulting transient is used for programming an arbitrary function generator (LeCroy, model 9109). The transient is amplified [ENI, model 2100 L] and coupled into two opposite segments of the ring electrode with a 180° phase shift.

For future experiments that may require a large number of cluster ions, e.g., the study of cluster–cluster collisions,[34] multiple cluster bunches may be injected and accumulated in the Penning trap:[35] After injection of a cluster bunch, the axial energy of the captured clusters is dissipated by collisions with rare gas atoms. For the next injection cycle, the potential of the entrance endcap is partially lowered to an extent that allows capture of incoming clusters and at the same time prevents previously stored clusters from escaping the trap. Due to the gas collisions, however, the magnetron radii increase and the clusters are lost from the trap. A technique to avoid this ion loss is quadrupole excitation of ions at their respective true cyclotron frequencies ν_c and concomitant buffer gas cooling.[36–38] Thus, the magnetron motion is continuously converted into cyclotron motion. The high velocity of the cyclotron motion provides for a rapid cooling and shrinking of the ion orbit due to gas collisions (overcoming the collisional expansion of the magnetron radius). Eventually, the desired cluster sizes are centered in the trap, whereas all other clusters are successively lost due to the increasing magnetron orbits.[35] The rf signals necessary for excitation of the ion motion are provided by frequency generators (Hewlett Packard, model 3325B; Stanford Research Systems, model DS345) coupled to four segments of the ring electrode.

VI. ION DETECTION

To study reactions of stored clusters the detection of products requires either a high mass resolution or a high sensitivity or a combination thereof. An unambiguous iden-

Downloaded 14 Mar 2003 to 137.138.124.154. Redistribution subject to AIP license or copyright, see http://ojps.aip.org/rsio/rsicr.jsp

tification of products from reactions, e.g., between metal clusters and gaseous molecules, calls for a mass resolving power of 10^3–10^4. On the other hand, for studies of photon induced cluster fragmentations a mass resolving power of only 100 is required. Finally, a high detection sensitivity is necessary to observe reaction or decay channels with small branching ratios. Fourier transform–ion cyclotron resonance (FT–ICR), which involves excitation and detection of the characteristic frequencies of the ions in the trap, provides high mass resolving power but limited detection efficiency, whereas time-of-flight (TOF) mass spectrometry after axial ejection of ions from the trap is highly sensitive but of low resolving power. Below, a technique is described, which combines rf excitation of ions inside the trap with TOF detection resulting in both high resolving power and sensitivity.

A. FT–ICR

FT–ICR mass spectrometry is a well-established method for the analysis of ion ensembles confined in ICR cells. We will therefore only give a short description and note some aspects relevant for our investigations. A more detailed outline of FT–ICR technique developments at the present apparatus is given in Refs. 23, 24, 39, and 40. Other developments of FT–ICR techniques and applications thereof have been summarized in Refs. 41 and 42.

Stored ions are excited by an electric dipole rf field to perform coherent cyclotron motions at frequencies ν_+. The amplitude of the rf voltage is limited to values low enough to avoid collisions of ions with the ring electrode. The excitation induces time-varying image charges in the ring electrode which are amplified, digitized, and stored in a transient recorder. Upon Fourier transformation a spectrum of ν_+ frequencies is obtained which is used to calculate ion masses via Eq. (5) and with signal amplitudes proportional to the number of ions. To improve the signal-to-noise (S/N) ratio several transients may be added prior to Fourier transformation. The S/N ratio increases with the square root of the number of added transient signals. During a FT–ICR mass analysis the ions remain inside the trap and may subsequently be used for further experiment.[43] The major advantage of FT–ICR, however, is its very high resolving power as examplified in Fig. 7. On the other hand, some hundreds of ions are needed to produce signals of a sufficiently large S/N ratio for routine measurements (Ref. 44 and below). This constitutes a severe drawback for experiments with only a small number of product ions. We have therefore implemented a new detection and mass analysis scheme for ICR cells: TOF after axial ejection of ions from the trap.

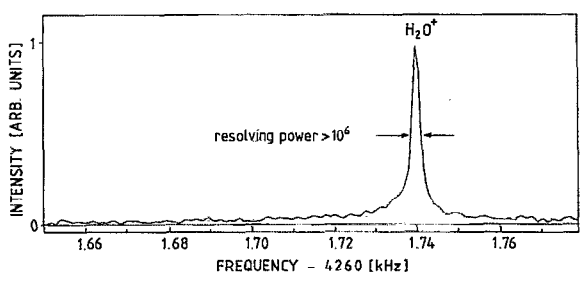

FIG. 7. High resolution FT–ICR spectrum of H_2O^+. The ions were produced inside the trap by electron impact ionization.

B. TOF

In this case, the ions stored in the trap are axially ejected (Fig. 8). Mass determination is performed by a measurement of the drift duration of the ejected ions to a detector. The time-of-flight resolution of ions ejected out of the trap is limited by the spatial and axial-energy distributions of the ions in the trap. The influence of the finite spatial distribution, caused by the axial oscillations of the ions, can be corrected by two accelerating stages of the spectrometer put to appropriate potentials.[45] For this purpose the Penning trap operates as the first stage and the electric field between the exit endcap and the extraction tube [Fig. 8(b)] provides the second stage. For ejection of positive ions, e.g., the potential of the entrance endcap, ϕ_{EC1}, is increased within 50 ns by 30–50 V. The potential of the exit endcap, ϕ_{EC2}, is decreased by the same amount (with respect to the ring electrode) to provide an electric field as homogeneous as possible inside the trap. The second acceleration stage is obtained by simultaneously lowering the potential of the extraction tube (25 mm from the center of the trap), which is kept at ϕ_{EC2} during

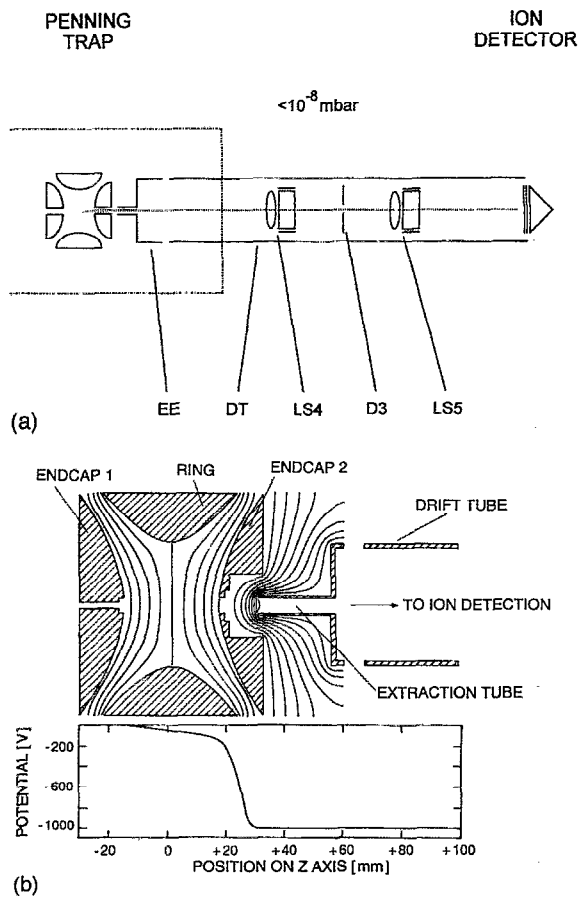

FIG. 8. (a) Outline of the time-of-flight section of the Penning trap mass spectrometer consisting of an extraction electrode and a drift tube with two lens/deflector pairs and a microchannel plate detector. LS and D as in Fig. 4; EE: extraction electrode; DT: drift tube. (b) Upper part: Blow-up of electrode geometry and equipotential lines of the electric field for time-of-flight detection of positive ions. Lower part: Potential along the z axis.

Downloaded 14 Mar 2003 to 137.138.124.154. Redistribution subject to AIP license or copyright, see http://ojps.aip.org/rsio/rsicr.jsp

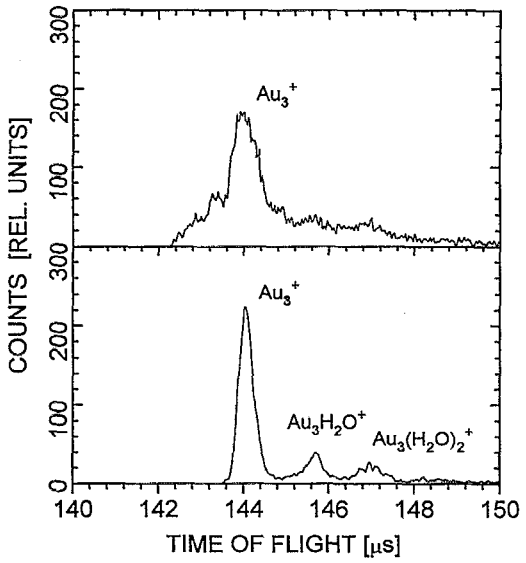

FIG. 9. Time-of-flight spectra of stored Au_3^+ ions. Upper part: Without buffer gas cooling, the mass resolving power is $m/\Delta m$(FWHM)≈85. Lower part: With buffer gas cooling at a pressure of 10^{-6}–10^{-5} mbar a resolving power of 225 is obtained.

ion storage, to the drift tube value of typically −400 to −1000 V.

Ion detection is performed with a tandem microchannel plate detector (MCP) mounted on axis at the end of the 2-m drift tube. The detection efficiency is assumed to be 30%. (A value of 50% was measured for 5.5-MeV α particles. The efficiency for heavier ions is likely to be somewhat lower.) The ion beam is directed towards the detector by two lenses and two pairs of deflection plates [Fig. 8(a)]. The diameter of the ion beam at 2/3 of the distance between trap and detector was investigated with a variable-size diaphragm and was determined to be below 5 mm. The mass resolution has been measured to be $m/\Delta m$(FWHM)=85 (Fig. 9, upper part) in the mass range 10–10 000 amu and at a trap potential of $U=3$ V. An improved resolution is obtained after narrowing the spatial and axial-energy distributions. This is achieved by collisions of the ions with argon atoms for times of ≅500 ms at a pressure of $(1\text{–}3)\times10^{-6}$ mbar. An improvement of the mass resolution up to $m/\Delta m$(FWHM)=225 (Fig. 9, lower part) has been determined. Such a resolving power is sufficient to distinguish between the different sizes of small homogeneous clusters, such as Au_n^+ $(n=2,3\ldots,23)$ as, e.g., investigated in Refs. 46–48.

C. Combination of rf excitation and TOF

In cases where the TOF technique has not enough resolving power and at the same time FT–ICR is not sensitive enough, the two approaches may be combined by monitoring the TOF signal as a function of rf excitation. Two methods may be distinguished.

(i) Radial ejection of the ions of interest: Suppose a TOF signal consists of several ion species all present in one unresolved peak. The ions under investigation are radially ejected by rf excitation at their reduced cyclotron frequency ν_+. The difference of the peak integrals of measurements

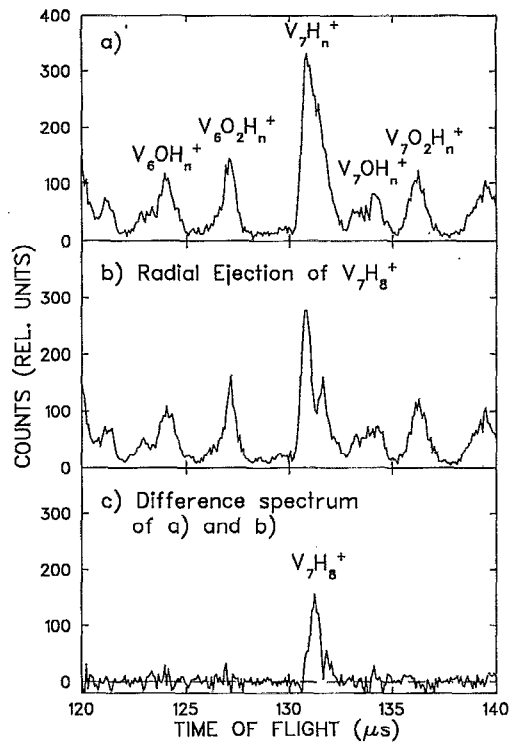

FIG. 10. Time-of-flight spectra of product ions from the reaction $V_n^+ + H_2$ at a storage time of 800 ms and a pressure of 3.7×10^{-6} mbar (a) without rf excitation and (b) with rf excitation and radial ejection of $V_7H_8^+$. (c) Difference of (a) and (b) which corresponds to the signal of $V_7H_8^+$.

without and with radial ejection gives the count rate of interest. This method is most reliable when the ions of interest are the dominant component of all the ion species. Otherwise, the complementary procedure is to be preferred.

(ii) Ejection of all ion species except the one under consideration: If only one ionic mass is exempted from radial ejection this will be the only one to yield a TOF signal.

For method (i) single-frequency excitation is sufficient. For method (ii) broadband excitation modes have to be utilized, i.e., excitation in frequency ranges both lower and higher than the reduced cyclotron frequency of the ions of interest. Figure 10 depicts an example for method (i): A TOF spectrum of reaction products $V_7H_n^+$ $(n=4,\ldots,10)$ from the interaction of V_7^+ clusters with H_2 at a pressure of 3.7×10^{-6} mbar and a reaction time of 800 ms [Fig. 10(a)]. Radial ejection of $V_7H_8^+$ results in the spectrum of Fig. 10(b). The difference of the two spectra shown in Fig. 10(c) represents the signal of the $V_7H_8^+$ cluster ions under investigation. The rf mass resolving power is limited by the slope of the frequency distribution of the rf power. For a typical excitation duration of $T_{rf}=10$ ms and an ion mass of 1000 amu ($\nu_+=76.5$ kHz), the resolving power is $m/\Delta m$(FWHM)$\cong T_{rf}\cdot\nu_+<765$.

VII. VACUUM SYSTEM AND SYSTEM ALIGNMENT

The vacuum system consists of four sections [cf. Figs. 4 and 8(a)] pumped independently and separated by valves. The laser vaporization source for the production of metal cluster ions is mounted inside a vacuum chamber evacuated by a turbomolecular pump (Balzers TPH 2200, 2200 ℓ/s).

Downloaded 14 Mar 2003 to 137.138.124.154. Redistribution subject to AIP license or copyright, see http://ojps.aip.org/rsio/rsicr.jsp

During operation, helium pulses are admitted into the cluster source at a rate of 10 Hz resulting in a pressure inside the vacuum chamber of about 10^{-4} mbar. The next section starts with a 6-cm region enclosed between two homebuilt skimmers with 1-mm holes for differential pumping. The region is evacuated by a diffusion pump (Balzers DIF 160 I, 650 ℓ/s) yielding a pressure of some 10^{-6} mbar during operation of the ion source.

The transfer section following the second skimmer is evacuated by two diffusion pumps (Balzers DIF 160 I, 650 ℓ/s and DIF 100 I, 300 ℓ/s). The resulting pressure is approximately 5×10^{-8} mbar.

The vacuum section of the Penning trap ($<10^{-8}$ mbar) is evacuated by a turbomolecular pump (Alcatel 2063, 400 ℓ/s mounted on a tube of 1.5-m height for operation in a magnetic field below 10 mT and a kryo pump (Leybold RPK 1500, 1500 ℓ/s). The microchannel-plate detector is mounted in a separate section at the end of the TOF drift section for easy access and pumped by a turbomolecular pump (Balzers TPU 170, 170 ℓ/s).

In order to study ion-molecule reactions, gases can be admitted continuously to the vacuum system through a 6-mm-diam stainless-steel tube, which ends at the position of the Penning trap. Alternatively, gas pulses of >1 ms duration may be injected using a piezoelectric valve mounted next to the Penning trap.[35] The gas inlet system consists of three storage vessels to allow the production of gas mixtures. In addition, the vapor pressure of room-temperature liquids may be used as well. Experiments are typically performed in a pressure range of 10^{-8}–10^{-5} mbar.

The ion capture in the trap without significant initial cyclotron energy and the ejection of ions for TOF analysis both critically depend on the alignment of the axes of the ion beam with respect to the magnetic field. For proper geometry, all components are mounted on disks centered inside the beam tube. The tube itself was aligned by use of a HeNe laser. The axis of the magnetic field was adjusted relative to the axis of the vacuum tube by installing an electron gun at the trap position and two collimator systems at 30-cm distance on both sides. The superconducting magnet and, in turn, the magnetic field axis was tilted until the electrons hit the two collimator systems in the center.

VIII. EXPERIMENT CONTROL AND DATA ANALYSIS

The various trigger signals and gates, e.g., for firing the vaporization laser, for switching the potentials of the Penning trap during ion injection and ejection, for the application of rf exitation, and for starting the data acquisition, are delivered by two homebuilt CAMAC memory modules. The units have 12 independent channels providing TTL pulses with adjustable widths and delays from 4 μs up to 1072 s. A typical time structure for an experiment with TOF analysis [collision induced dissociation of Au_n^+ (Refs. 46–48)]—which consists of ion creation, capture in the trap, collisions with rare gases, and product analysis—is shown in Fig. 11. Gold clusters are produced by laser vaporization (a), transferred to the Penning trap and captured (b). During the storage time (c), a cluster of given size is mass selected (d) and accelerated (e) to induce collisions with rare gas atoms. After

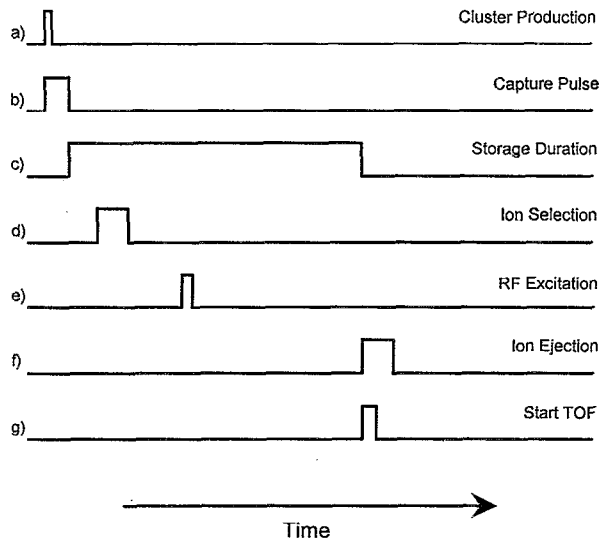

FIG. 11. Typical timing sequence for one measurement cycle of a time-of-flight experiment. For details see text.

collision induced dissociation the product ions are ejected out of the trap (f) and the data acquisition is started (g) to record the signals of the multichannel plate detector mounted at the end of the TOF drift tube. From the amplified detector pulses standard NIM pulses are produced by a discriminator. The NIM pulses are registered by a transient recorder (consisting of a LeCroy module TR8818 and two modules MM8103A). A TOF spectrum of (typically) 16 k data points is obtained by stepping the addresses of the transient recorder at variable frequencies up to 100 MHz.

The timing sequence for a FT–ICR experiment is similar, with a variation only during ion detection. In this case the cyclotron motion of ions is excited and an ICR transient of up to 64k data points is recorded before the trap is emptied for the next sequence.

An Eurocom-6 computer (Eltec) installed in a VME bus system is used for data taking and for programming the CAMAC electronic units and the arbitrary-function generator for SWIFT excitation. Transfer of 16k data points into computer memory is finished within less than 60 ms. Hence, experimental cycles based on TOF analysis can be repeated at a rate of up to 10 Hz. For FT–ICR analysis, the repetition rate of experimental cycles is limited by the duration of the transient signal to be recorded (typically 0.1–1 s). Fourier transformation of the transient signal is performed on a personal computer which is also used for the on-line display of the measured data and for the control of the experimental timing sequence via the VMEbus computer. Off-line data analysis is performed on DEC computers.

The rate of cluster ion production may fluctuate considerably and shows temporal drifts. Thus, it is crucial to normalize the measured product intensities with respect to the signal of the precursors (i.e., the number of injected clusters). This is achieved by programming the memory modules with different timing cycles: One module delivers a reduced time structure of the experimental sequence including only ion creation, storage, ejection, and detection. The second module includes an additional step which triggers the interactions

Downloaded 14 Mar 2003 to 137.138.124.154. Redistribution subject to AIP license or copyright, see http://ojps.aip.org/rsio/rsicr.jsp

under investigation (e.g., reactions with gaseous atoms or a laser beam). The two timing cycles are repeated alternately and the respective data are stored in different sections of computer memory. This method allows the quasisimultaneous observations of precursor and product ions.

IX. SELECTED RESULTS

A. Ion trap techniques

An important parameter for investigations of high-mass ions, such as biomolecules or clusters, is the critical mass up to which ions can be stored in Penning or ICR traps. The motions of ions with higher mass-to-charge ratios are unstable and they are therefore lost from the trap immediately after creation or capture. The critical mass is inversely proportional to the trap potential: $m_{\mathrm{crit}}=qB^2d^2/(2U)$. This mass limit, as well as instabilities of the ion motion, were studied with Au_n^- clusters.[30] At a trap potential of $U=8.2$ V, clusters up to Au_{145}^- ($m/q\cong 28\ 000$ u/e) were stored.

As explained in the previous section, different experimental cycles can be executed alternately for subsequent pulses of the vaporization laser. This allows the detection of ions alternately by the TOF and the FT–ICR techniques. Thus, it is feasible to calibrate the FT–ICR signal height with respect to the number of ions counted by TOF mass spectrometry: Fig. 12(a) shows a FT–ICR spectrum of a single transient for Au_5^+ clusters with a signal three times higher than the noise level. From the alternately recorded TOF spectrum, the number of ions causing the signal was determined as 170. This number was calculated based on a microchannel plate efficiency of 30% and assuming that no ions are lost along the drift path from the trap to the detector. This is a reasonable assumption since the beam diameter after 2/3 of the drift path is below 5 mm, which was determined with a diaphragm of variable opening. The number obtained above agrees with calculations based on FT–ICR data alone.[44]

The minimum number of stored ions that is required for FT–ICR detection can be decreased by accumulation of several transient spectra prior to Fourier transformation. Figures 12(b) and 12(c) display FT–ICR and TOF spectra of Au_5^+ clusters obtained by adding 125 transient spectra. In this case the minimum number of ions per transient is 15 for a FT–ICR signal-to-noise ratio larger than three. Note, that adding of transients before Fourier transformation yields an improvement of the signal-to-noise ratio which scales with the square root of the number of added transients. Upon accumulation of a number of ion bunches prior to recording a transient spectrum the signal-to-noise improvement is even larger. It is proportional to the number of ion bunches.[35]

B. Cluster experiments

In this section we give an overview of the experiments which focus on the physical and chemical properties of metal clusters. Further results are summarized in Ref. 29. As a first application of the setup to cluster investigations the fragmentation of gold clusters, Au_n^+ ($n=2,\ldots,23$) induced by collisions with krypton and xenon, was studied at collision energies of 10–200 eV.[46–48] Clusters with an even number of

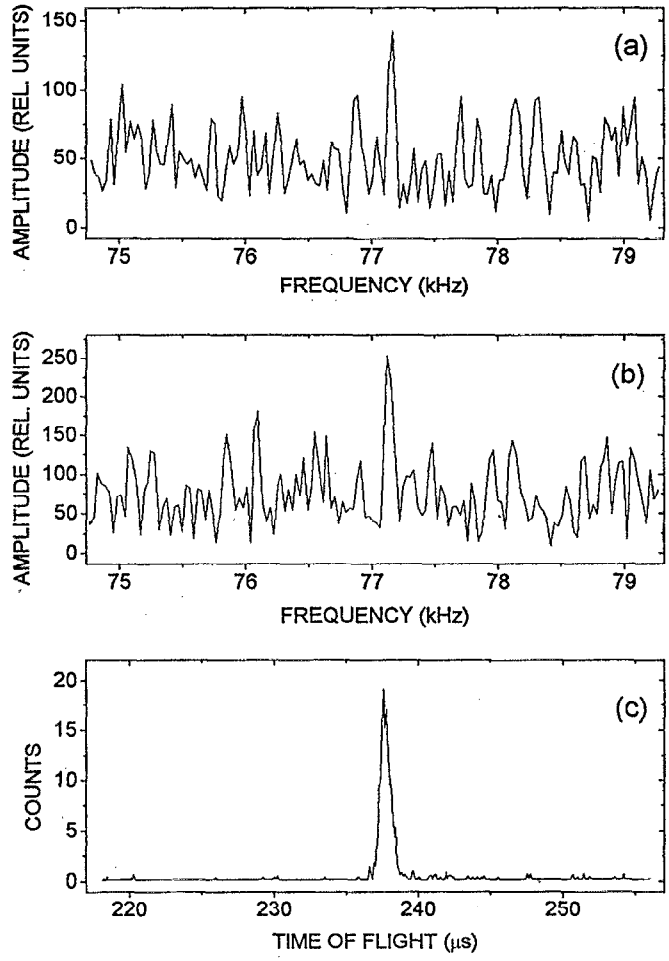

FIG. 12. Detection of Au_5^+ clusters by FT–ICR and time-of-flight mass spectrometry. (a) FT–ICR spectrum of one transient signal (at $\nu_+\approx 77\ 170$ Hz) produced by 170 ions. (b) FT–ICR spectrum of the sum of 125 transient signals produced by 15 ions per transient. (c) TOF spectrum recorded alternately with (b) for calibration of the number of ions (see text).

valence electrons were found to have higher threshold energies for fragmentation as compared to their odd-electron counterparts. This is in line with the observation that (for Au_n^+, $n<16$) clusters with an even number of electrons largely decay by the emission of dimers whereas odd-electron clusters decay by monomer emission. A similar odd–even intensity alternation has been observed for small gold cluster ions produced by sputtering techniques.[49]

Interations between clusters and molecules were studied for the system $Au_n^+ + N_2O$. On bulk gold surfaces, the N_2O molecule is known to decompose by a catalytical activation.[50] Reaction studies between Au_n^+ ($n=1,\ldots,4$) and N_2O were carried out in order to probe whether N_2O decomposition is already induced by these microscopic systems and whether their electronic structure influences the reaction pathway.[31] The activation energy involved in the cluster-mediated decomposition was found to be lower as compared to decomposition on a bulk surface. Also, product ions with an even number of valence electrons, e.g., Au_1O^+, Au_2N^+, and Au_3O^+, were formed rather than the odd-electron species.

The long observation durations accessible with the stor-

Downloaded 14 Mar 2003 to 137.138.124.154. Redistribution subject to AIP license or copyright, see http://ojps.aip.org/rsio/rsicr.jsp

age of ions were further exploited in an investigation of the thermionic electron emission of W_n^- clusters ($n=4-14$ and 18–20) induced by photoexcitation.[51] The cohesive energy of W_n^- clusters is larger than the electron affinity. Hence, electron emission dominates over the evaporation of atoms. Thermionic emission was observed on a time scale of 1–500 ms which indicates a statistical equilibration of the excitation energy.

For gold and silver the cohesive energy is lower and the de-excitation of clusters can be monitored via emission of atoms and dimers. The clusters Ag_{21}^+, Au_9^+, and Au_{21}^+ were irradiated with photons of 3.8–4.4 eV energy. As already observed by collision-induced dissociation of Au_n^+ clusters, even-electron clusters preferably decay by dimer emission whereas odd-electron clusters decay by monomer emission.[52] The measured lifetimes after photon absorption extend from a few microseconds up to several milliseconds,[53] indicating again a statistical distribution of the excitation energy over the vibrational degrees of freedom. The examples show that the Penning trap system is an appropriate device for the study of the long-term behavior of cluster ions.

ACKNOWLEDGMENTS

The experiments have been supported by the Deutsche Forschungsgemeinschaft, the Materialwissenschaftliche Forschungszentrum of the Johannes Gutenberg-Universität, Mainz, and the SCIENCE program of the European Community. K.D. acknowledges financial support provided by the Indo-German Collaboration between the Bhabha Atomic Research Centre, Bombay, and the Internationales Büro, KFA Jülich, Germany. S. K. acknowledges financial support by the Deutsche Akademische Austrauschdienst (DAAD). We thank D. Gerlich for his help during the construction of the piezo valve for the pusled gas inlet as well as D. Kreisle and H. Weidele for their help in constructing the laser vaporization source.

[1] W. A. deHeer, Rev. Mod. Phys. **65**, 611 (1993).
[2] J. Allison and R. M. Stepnowski, Anal. Chem. **59**, 1072A (1987).
[3] Proc. Workshop on Physics with Penning Traps, edited by G. Bollen and C. Carlberg, Lertorpet, Sweden, 1991, Phys. Scr. RS 20 (1993).
[4] R. C. Thompson, Meas. Sci. Technol. **1**, 93 (1990).
[5] J. F. J. Todd, Mass Spectrom. Rev. **10**, 3 (1991).
[6] *Fourier Transform Mass Spectrometry*, edited by M. V. Buchanan (American Chemical Society, Washington D.C., 1987), ACS Symposium Series 359.
[7] G. Gabrielse, H. Dehmelt, and W. Kells, Phys. Rev. Lett. **54**, 537 (1985).
[8] R. S. Van Dyck, Jr., P. B. Schwinberg, and H. G. Dehmelt, Phys. Rev. Lett. **59**, 26 (1987).
[9] V. Natarajan, K. R. Boyce, F. DiFilippo, and D. E. Pritchard, Phys. Rev. Lett. **71**, 1998 (1993).
[10] F. L. Moore, L. S. Brown, D. L. Farnham, S. Jeon, P. B. Schwinberg, and R. S. Van Dyck, Jr., Phys. Rev. A **46**, 2653 (1992).
[11] J. Kern, T. Engel, D. Hagena, and G. Werth, Phys. Scr. **46**, 575 (1992).
[12] H. Stolzenberg, G. Audi, St. Becker, G. Bollen, F. Kern, H.-J. Kluge, R. B. Moore, Th. Otto, G. Savard, and L. Schweikhard, Phys. Rev. Lett. **65**, 3104 (1990).
[13] G. Gabrielse, X. Fei, L. A. Orozco, R. L. Tjoelker, J. Haas, H. Kalinowsky, T. A. Trainor, and W. Kells, Phys. Rev. Lett. **65**, 1317 (1990).
[14] K. Eller and H. Schwarz, Chem. Rev. **91**, 1121 (1991).
[15] J. M. Alford, P. E. Williams, D. J. Trevor, and R. E. Smalley, Int. J. Mass Spectrom. Ion Proc. **72**, 33 (1986).
[16] M. P. Irion and A. Selinger, Chem. Phys. Lett. **158**, 145 (1989).
[17] D. Gerlich and S. Horning, Chem. Rev. **92**, 1509 (1992).
[18] *Quadrupole Mass Spectrometry and its Applications*, edited by P. H. Dawson (Elsevier, Amsterdam, 1976).
[19] R. E. March and R. J. Hughes, *Quadrupole Storage Mass Spectrometry* (Wiley, New York, 1989).
[20] L. S. Brown and G. Gabrielse, Rev. Mod. Phys. **58**, 233 (1986).
[21] M. W. Senko and F. W. McLafferty, Annu. Rev. Biophys. Biomol. Struct. **23**, 763 (1994).
[22] S. M. Michael, M. Chien, and D. M. Lubman, Rev. Sci. Instrum. **63**, 4277 (1992).
[23] L. Schweikhard, M. Lindinger, and H.-J. Kluge, Int. J. Mass Spectrom. Ion Proc. **98**, 25 (1990).
[24] L. Schweikhard, M. Lindinger, and H.-J. Kluge, Rev. Sci. Instrum. **61**, 1055 (1990).
[25] R. D. Knight, Int. J. Mass Spectrom. Ion Phys. **51**, 127 (1983).
[26] H. G. Dehmelt, Adv. At. Mol. Phys. **3**, 53 (1967).
[27] D. E. Powers, S. H. Hansen, M. E. Geusig, A. C. Puiu, J. B. Hopkins, T. G. Dietz, M. A. Duncan, P. R. R. Langridge-Smith, and R. E. Smalley, J. Phys. Chem. **86**, 2556 (1982).
[28] H. Weidele, U. Frenzel, T. Leisner, and D. Kreisle, Z. Phys. D **20**, 425 (1991).
[29] L. Schweikhard *et al.*, Phys. Scr. (in press).
[30] L. Schweikhard, J. Ziegler, H. Bopp, and K. Lützenkirchen, Int. J. Mass Spectrom. Ion Proc. **141**, 77 (1995).
[31] G. Dietrich, K. Lützenkirchen, St. Becker, H.-U. Hasse, H.-J. Kluge, M. Lindinger, L. Schweikhard, J. Ziegler, and S. Kuznetsov, Ber. Bunsenges. Phys. Chem. **98**, 1608 (1994).
[32] H. Schnatz, G. Bollen, P. Dabkievicz, P. Egelhof, F. Kern, H. Kalinowsky, L. Schweikhard, H. Stolzenberg, and H.-J. Kluge, The ISOLDE Collaboration, Nucl. Instrum. Methods A **251**, 17 (1986).
[33] A. G. Marshall, T. C. L. Wang, and T. L. Ricca, J. Am. Chem. Soc. **107**, 7893 (1985).
[34] R. Schmidt, G. Seifert, and H. O. Lutz, Phys. Lett. A **158**, 231 (1991).
[35] H.-U. Hasse, St. Becker, G. Dietrich, N. Klisch, H.-J. Kluge, M. Lindinger, K. Lützenkirchen, L. Schweikhard, and J. Ziegler, Int. J. Mass Spectrom. Ion Proc. **132**, 181 (1994).
[36] G. Savard, St. Becker, G. Bollen, H.-J. Kluge, R. B. Moore, L. Schweikhard, H. Stolzenberg, and U. Wiess, Phys. Lett. A **158**, 247 (1991).
[37] L. Schweikhard, S. Guan, and A. G. Marshall, Int. J. Mass Spectrom. Ion Proc. **120**, 71 (1992).
[38] S. Guan, H. S. Kim, A. G. Marshall, N. C. Wahl, T. D. Wood, and X. Xiang, Chem. Rev. **94**, 2161 (1994).
[39] L. Schweikhard, Rapid Commun. Mass Spectrom. **4**, 360 (1990).
[40] L. Schweikhard, Int. J. Mass Spectrom. Ion Proc. **107**, 281 (1991).
[41] A. G. Marshall, and L. Schweikhard, Int. J. Mass Spectrom. Ion Proc. **118/119**, 37 (1992).
[42] *FT-ICR/MS Analytical Applications of Fourier Transform Ion Cyclotron Resonance Mass Spectrometry*, edited by B. Asamoto (VCH, Weinheim, 1991).
[43] E. R. Williams, K. D. Henry, and F. W. McLafferty, J. Am. Chem. Soc. **112**, 6157 (1990).
[44] P. A. Limbach, P. B. Grosshans, and A. G. Marshall, Anal. Chem. **65**, 135 (1993).
[45] W. C. Wiley and I. H. McLaren, Rev. Sci. Instrum. **26**, 1150 (1955).
[46] St. Becker *et al.*, Z. Phys. D **30**, 341 (1994).
[47] St. Becker *et al.*, Rapid Commun. Mass Spectrom. **8**, 401 (1994).
[48] St. Becker *et al.*, Comp. Mat. Sci. **2**, 633 (1994).
[49] A. Selinger, P. Schnabel, W. Wiese, and M. P. Irion, Ber. Bunsenges, Phys. Chem. **94**, 1278 (1990).
[50] D. D. Eley and C. F. Knights, Proc. R. Soc. London, Ser. A **294**, 1 (1966).
[51] H. Weidele, St. Becker, H.-J. Kluge, M. Lindinger, L. Schweikhard, C. Walther, J. Ziegler, and D. Kreisle, Surf. Rev. Lett. (in press).
[52] C. Walther, Diploma thesis, Mainz (1994), publication in preparation.
[53] M. Lindinger, Ph.D. thesis, Mainz (1995), publication in preparation.

Downloaded 14 Mar 2003 to 137.138.124.154. Redistribution subject to AIP license or copyright, see http://ojps.aip.org/rsio/rsicr.jsp